that UFSq should be useful as a photogeneration pigment in copier as well.

Electrical Cycling. To test the durability of UFSq in practical photoreceptor application, a bilayer device of UFSq (CH_2Cl_2 purified)[26] was subjected to a xerographic cycling test on an in-house drum scanner. The speed experienced by the device was $\sim$30 in./s. Basically, the device was subjected to thousands and thousands of charging–photodischarge cycles at a very high rate. In each cycle, the surface potential of the device at 0.2 s after charging, V_H, and the surface potential after light erasure (by a 300 ergs/cm^2 white light source), V_L, were recorded. The results of a 50 000 cycling plot are given in Figure 7. Our data clearly indicate that UFSq is extremely stable electrically. The suitability of using UFSq in practical devices is demonstrated.

Concluding Remarks

This report summarizes results of our investigation on the synthesis, purification, and xerographic properties of UFSq. UFSq can be synthesized by either direct or indirect condensation of 1-(3′,4′-dimethoxyphenyl)-2-hydroxycyclobutene-3,4-dione with 3-fluoro-*N*,*N*-dimethylaniline. Xerographic evaluation showed that the as-synthesized UFSq exhibits a dark decay of −30 V/s and $E_{0.5}$ values of 4.3–6.8 ergs/cm^2 in bilayer photoreceptor devices. Purification of UFSq by solvent extraction, particularly with methylene chloride, improves the purity and consequently the xerographic properties of UFSq. A dark-decay value of −15 V/s and $E_{0.5}$ values of 3.1 and 1.9 ergs/cm^2 at 600 and 790 nm, respectively, have been obtained. Evidence has been obtained that the improvements in xerographic properties may be a combination of the high purity and the high hole-injection efficiency of UFSq, from the CGL to the CTL, in the xerographic device.

A device of UFSq is shown to have panchromatic response from the visible to the near-IR regions as well as excellent 50K cyclic stability. This performance makes UFSq one of the most sensitive panchromatic (visible-IR regions) organic photoconductors known to date, rendering the potential use of UFSq in printers, copiers, and multifunction printer-copiers.

Acknowledgment. I thank F. C. Bailey for his assistance in synthesizing some of the precursors used in this work. Thanks are also due to M. Evan and M. Curtis for X-ray powder diffraction patterns, W. Niedzialkowski for the SEM micrographs, and S. Towers for the cycling experiments.

Registry No. TPD, 65181-78-4; UFSq, 140175-46-8; FC_6H_4-*m*-NMe_2, 2107-43-9; CH_2Cl_2, 75-09-2; 1-(3′,4′-dimethoxyphenyl)-2-hydroxycyclobutene-3,4-dione, 126605-20-7.

---

(26) In the cycling test, a titanized mylar substrate was used in place of the ball-grain aluminum substrate.

Heterophasic Isotope Exchange in Nanoscale Metal Oxide Particles. Lattice Oxygen and Surface OH Groups with Water Vapor (D_2O and $H_2{}^{18}O$)

Yong-Xi Li and Kenneth J. Klabunde*

Department of Chemistry, Kansas State University, Manhattan, Kansas 66506

Received October 29, 1991. Revised Manuscript Received February 21, 1992

Ionic solids MgO, CaO, and Fe_2O_3 exchange surface and lattice oxide anions with $H_2{}^{18}O$ as monitored by pulsed reactor–GC-MS studies. Depending on the temperature, the process can be controlled to exchange only OH, or additional surface lattice O^{2-}, or additionally, interior lattice O^{2-} (up to 16 layers deep). Exchange of surface oxide has an activation energy 5 times lower than exchange of bulk-lattice oxide, and the latter is probably controlled by E_a(diffusion). High surface area, small particle size MgO samples exchange most readily. Exchange studies with D_2O have shown that surface OH can be quantitated by the same pulsed reaction–GC-MS technique. These experiments have allowed the synthesis of isotopically labeled $Mg^{18}O$, which has proven useful for clarifying surface adsorption/decomposition chemistry. An example is given where the $Mg^{18}O$ yielded labeled formic acid in the surface decomposition of an organophosphorus compound, proving that surface and lattice oxide can take part in such adsorption/decomposition processes.

Introduction

In a series of reports on the adsorption/decomposition of organophosphorus compounds on nanoscale MgO particles, it was determined that surface hydroxyl groups as well as lattice oxygen play a role.[1-3] Furthermore, the importance of surface OH in many catalytic processes on basic metal oxide surfaces should not be minimized.[4-6] Due to the importance of surface OH and possibly lattice oxygen (oxide anions on the surface and in the interior of the bulk) on these adsorption/decomposition/catalytic processes, we decided to investigate isotope exchange of deuterium and water-^{18}O with MgO, CaO, and Fe_2O_3 nanoscale particles, and we report the results herein.

Before presenting these results, some related work should be summarized. Indeed, the mobility of lattice oxygen in oxidation catalysts has been studied in depth, and these studies have shown that for some multivalent

---

(1) Li, Yong-Xi; Klabunde, K. J. *Langmuir* **1991**, *7*, 1388.
(2) Li, Yong-Xi; Klabunde, K. J. *Langmuir* **1991**, *7*, 1394.
(3) Li, Yong-Xi; Kopper, O.; Maher, A.; Klabunde, K. J. *Chem. Mater.*, in press.
(4) Larson, J. G.; Hall, W. K. *J. Phys. Chem.* **1965**, *69*, 3080.
(5) Lemberton, J. L.; Perot, G.; Guisnet, M. *J. Catal.* **1984**, *89*, 69.
(6) Hoq, M. F.; Nieves, I.; Klabunde, K. J. *J. Catal.* **1990**, *123*, 349 references therein.

0897-4756/92/2804-0611$03.00/0

metal oxides, the crystal lattice can serve as a reservoir for oxygen, storing O^{2-} and releasing O_2 under appropriate conditions.[7-10] In fact this is a necessary property of many oxidation catalysts, and so it might be expected that lattice oxygen isotope exchange would be energetically feasible. Early work of Winter[11-14] showed that for PbO, PdO, AgO, and CuO the surface oxygen could be exchanged with gaseous O_2. For Na_2WO_4, V_2O_5, MoO_3, and WO_3 all of the lattice oxygen could be exchanged with gaseous O_2. However, SiO_2 and GeO_2 were inactive in this exchange under the same conditions. Winter,[11-14] Boreskov,[15] and Klier and co-workers[16] have proposed possible mechanisms based on kinetic studies.

Several transition metal oxides have also come under scrutiny regarding lattice oxygen/O_2 exchange.[17-23] Supported metallic catalysts are also of interest. For example, White and co-workers investigated Pt/CeO_2 and found that lattice oxygen played an important role in CO oxidation.[20] Cant, Peil, and their co-workers investigated the rates of various oxygen isotope transfer processes over Li^+/MgO catalysts in a flow system for the oxidative coupling of methane.[24,25] Both surface and lattice oxygen participated during the oxidation of methane with O_2. Oxide exchange with O_2 was also detected with supported V_2O_5 catalysts,[26,27] and recently Cunningham and Healy examined O_2 and H_2 exchange on CaO.[28] They found that surface OH did undergo exchange with O_2 at 350 °C, while at 425–500 °C surface oxide also exchanged.

It is important to note that essentially all oxide exchange studies have dealt with oxide/O_2. To our knowledge, oxide/H_2O exchange studies have not been reported. In the studies reported herein, exchange of surface OH and lattice O^{2-} occurred more readily with $H_2{}^{18}O$ than with ${}^{18}O_2$, a finding that could be important for many systems of interest.

Experimental Section

(1) Metal Oxides. Two kinds of MgO were used in this study: MgO of about 130 m^2/g prepared by pyrolysis of $Mg(OH)_2$ which we refer to as MgO(130), and MgO of about 390 m^2/g prepared by an aerogel/autoclave procedure which we refer to as MgO(390).[1-3] Samples of CaO(120) and α-Fe_2O_3(140) were also prepared and tested. All surface areas were determined by the BET method using nitrogen.

(2) Water. The exchange reactions carried out employed D_2O (99.8 atom % D) from Aldrich Chemical Co. and $H_2{}^{18}O$ (99% ${}^{18}O$) from ISOTEC, Inc.

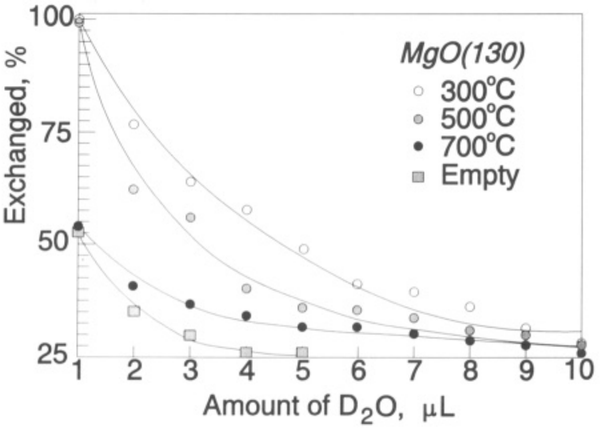

Figure 1. Amounts of D_2O exchanged on MgO(130) at different temperatures. "Empty" means no MgO sample in the reactor; the curve for D_2O exchange in the empty reactor represents background. At 300 °C, much more D_2O exchanged compared with that at 700 °C, which indicates more OH groups on the surface of the MgO(130) at 300 °C.

(3) Reactor GC-MS System and Procedure. A in situ reactor GC-MS system was utilized as previously described.[3] The helium carrier gas was passed through a 5-Å zeolite column and then passed through the U-tube reactor that contained 0.1 g of metal oxide powder. The flow rate was usually 50 mL/min. The oxide was heated to the desired temperature, and helium flowed over it for at least 2 h before injections of D_2O or $H_2{}^{18}O$ were commenced.

Injections of 1 μL of D_2O or H_2O^{18} were initiated and the effluent of each injection studied by GC-MS. The fractions of H_2O, HOD, D_2O or H_2O or $H_2{}^{18}O$ were determined for each injection. For hydrogen exchange the reaction of $D_2O(v)$ (v = vapor) and $HO^-(s)$ (s = solid) were assumed to proceed as follows:

$$D_2O(v) + HO^-(s) \rightarrow HDO(v) + DO^-(s)$$

$$D_2O(v) + 2HO^-(s) \rightarrow H_2O(v) + 2DO^-(s)$$

the percent molar fraction of D can be obtained from the equation

$$f_D = \frac{2P_{20} + P_{19}}{2(P_{20} + P_{19} + P_{18})} \times 100 \qquad (1)$$

Here, P_{20}, P_{19}, and P_{18} are the relative peak heights at *m/e* 20, 19, and 18 in the MS spectrum. For oxygen exchange:

$$H_2{}^{18}O(v) + HO^-(s) \rightarrow H_2O(v) + H^{18}O^-(s)$$

$$H_2{}^{18}O(v) + MgO(s) \rightarrow H_2O(v) + Mg^{18}O(s)$$

The % molar fraction of ${}^{18}O$ can be obtained from

$$f_{18} = \frac{P_{20}}{P_{20} + P_{18}} \times 100 \qquad (2)$$

Here, P_{20} and P_{18} are relative peak heights at *m/e* 20 and 18 in the MS spectrum.

Results and Discussion

(1) D_2O Exchange. Figure 1 illustrates the results of exchange between D_2O vapor and hydroxyl groups on MgO(130). From the MS spectra the fraction f_D was calculated according to eq 1. The amount of D_2O that was exchanged with surface OH groups for each microliter of D_2O injected is plotted against the total number of microliters. Since the interior walls of the device contained small amounts of adsorbed water, an empty reactor was also examined in control experiments, and this exchangeable H_2O was subtracted out in the calculations.

Figure 1 illustrates that at the lower temperature (300 °C) the amount of D_2O consumed is highest. These results reflect the higher population of surface OH groups of

---

(7) Arnold III, E. W.; Sundaresan, S. *Chem. Eng. Comm.* **1987**, *58*, 213.
(8) Black, J. B.; Scott, J. D.; Serwicka, E. M.; Goodenough, J. B. *J. Catal.* **1987**, *106*, 16.
(9) Muzykantov, V. S. *React. Kinet. Catal. Lett.* **1987**, *35*, 437.
(10) Dadyburjor, D. B.; Ruckenstein, E. *J. Catal.* **1980**, *63*, 383.
(11) Winter, E. R. S. *J. Chem. Soc. A* **1968**, 2889.
(12) Winter, E. R. S. *J. Chem. Soc., Supplement I* **1964**, 5781.
(13) Winter, E. R. S. *J. Chem. Soc.* **1955**, 3824.
(14) Winter, E. R. S. *J. Chem. Soc.* **1954**, 1522.
(15) Boreskov, G. K. *Adv. Catal.* **1964**, *15*, 285.
(16) Klier, K.; Novakova, J.; Jiru, P. *J. Catal.* **1963**, *2*, 479.
(17) Lin, P.; Yu, M.; Okuhara, T.; Misono, M. *J. China Univ. Sci. Technol.* **1987**, *17* (2), 274.
(18) Haber, J.; Serwicka, E. M. *React. Kinet. Catal. Lett.* **1987**, *35*, 369.
(19) Zhan, X. L.; Kai, X.; Yu, Q. L.; Qi, X. B. *J. Catal.* **1989**, *119*, 249.
(20) Jin, T.; Okuhara, T.; Mains, G. J.; White, J. M. *J. Phys. Chem.* **1987**, *91*, 3310.
(21) Lashier, M. E.; Schader, G. L. *J. Catal.* **1991**, *128*, 113.
(22) Zhan, X. L.; Qi, X. B.; Nai, J. W. *J. Catal.* **1988**, *113*, 45.
(23) Sachtler, W. M. H.; Dorgelo, G. J. H.; Fahrenfort, J.; Voorhoeve, J. *Prepr., 4th Int. Cong. Catal., Moscow* **1968**.
(24) Cant, N. W.; Lukey, C. A.; Nelson, P. F. *J. Catal.* **1990**, *124*, 336.
(25) Peil, K. P.; Goodwin, Jr. J. G.; Marcelin, G. *J. Phys. Chem.* **1989**, *93*, 5977.
(26) Minachev, K. M.; Antoshin, G. V.; Klissurski, D. G.; Guin, N. K.; Abadzhijeva, N. T. *J. Chem. Soc., Faraday Trans. 1* **1979**, *75*, 691.
(27) Cunningham, J.; Goold, E. L.; Leahy, E. M. *J. Chem. Soc., Faraday Trans. 1* **1979**, *75*, 305.
(28) Cunningham, J.; Healy, C. P. *J. Chem. Soc., Faraday Trans 1* **1987**, *83*, 2973.

Table I. Amounts of D_2O Exchanged on Different Oxides at Different Temperatures[a]

	temp, °C	amt of D_2O used for 0.1 g of MgO sample Σ, μL	$\Sigma_T - \Sigma_{empty}$, μL	BET surf. area, m^2/g before	BET surf. area, m^2/g after	OH/nm^2[a]
empty tube		3.62				
MgO(130)	700	3.78	0.16	131	67	0.49
	500	4.73	1.11	127	114	2.8
	300	5.47	1.85	129	117	4.5
MgO(390)	300	9.64	6.02	381	301	5.3
CaO(120)	300	4.68	1.06	120	104	2.8
α-Fe_2O_3(140)	300	4.28	0.66	135	99	1.7

[a] Average surface area.

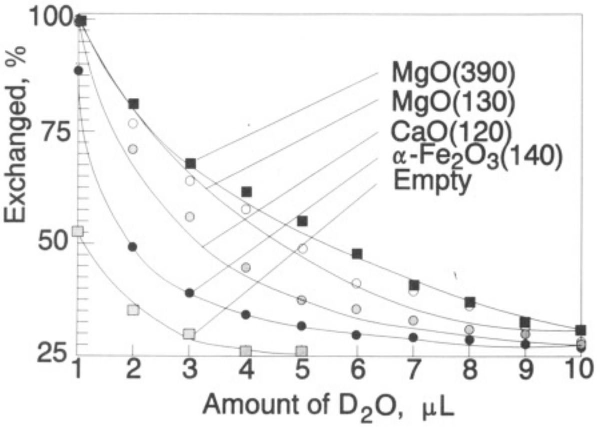

Figure 2. Amounts of D_2O exchanged on different oxides at 300 °C. The curve for MgO(390) is higher compared with curves of other oxides, which indicates more OH groups on the surface of the MgO(390) compared with the other oxides (see Table I).

MgO(130) heat treated at 300 °C.[1-3,29] High heat treatments led to progressively lower surface OH concentrations, and at 700 °C the amount of D_2O consumed was close to the control experiments (empty reactor). Table I summarizes these data and from which the number of surface OH/nm^2 was calculated in each case. These concentrations of surface OH groups are in general agreement with Et_3Al titrations we have carried out,[29] but of course the exact amounts depend on the particular experimental conditions of temperature, flow rate, etc. Note from Table I that at 700 °C, on average, only 0.49 OH/nm^2 were present, while at 300 °C about 10 times as many were present.

Figure 2 summarizes exchange results of different oxide samples at 300 °C. Obviously, on MgO(390) more D_2O exchange occurred, as would be expected for its higher starting surface area. Also note that CaO(120) and α-Fe_2O_3(140) possessed significantly lower OH concentrations. Overall, the concentrations of OH/nm^2 were found to be in the order MgO(390) > MgO(130) > CaO(120) > α-Fe_2O_3(140). Since surface OH groups are of great importance in surface adsorption/decomposition and catalytic schemes,[4-6] such data are of interest in their own right.

$H_2{}^{18}O$ Exchange. Pulses of $H_2{}^{18}O$ were passed over MgO(130) and MgO(390) samples and the results are shown in Figures 3 and 4. The exchange fraction f_{18} was calculated from eq 2. At 300 and 500 °C, the amount of $H_2{}^{18}O$ consumed was 2–3 times greater with MgO(390) than with MgO(130). However, at 700 °C the amounts of $H_2{}^{18}O$ consumed *were almost identical*. We attribute this to the fact that the surface areas of both samples decreased substantially at 700 °C in the presence of water vapor (Table II) and were nearly the same (87 and 71 m^2/g, respectively). Indeed, this sintering phenonemon, caused

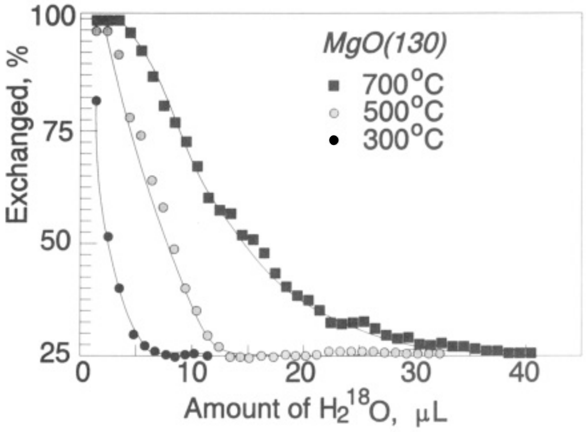

Figure 3. Amounts of $H_2{}^{18}O$ exchanged on MgO(130) at different temperatures. At 700 °C, much more $H_2{}^{18}O$ exchanged compared with 500 and 300 °C, which indicates that lattice oxygen is involved in the exchange reaction (not only surface OH groups).

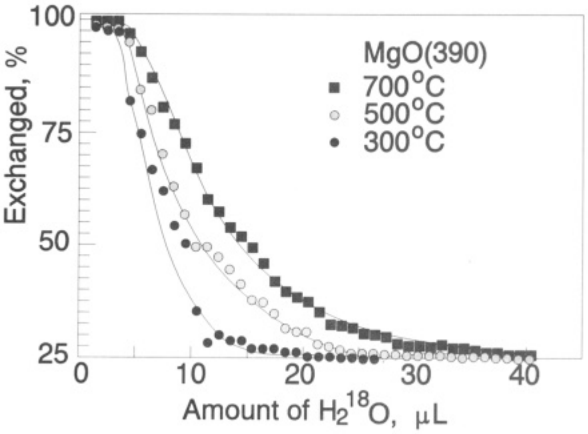

Figure 4. Amounts of $H_2{}^{18}O$ exchanged on MgO(390) at different temperatures. At 700 °C, more $H_2{}^{18}O$ exchanged compared with 500 and 300 °C, which indicates that lattice oxygen is involved in the exchange reaction. Moreover, the curve at 700 °C is located at almost the same position as that for MgO(130), which is because both samples had sintered to about the same surface area at this reactor temperature.

Table II. Amounts of $H_2{}^{18}O$ Exchanged on MgO(130) and MgO(390)

	temp, °C	$H_2{}^{18}O$, μL	surf. area, m^2/g (after use)	^{16}O exchange, % OH^-	^{16}O exchange, % ^{16}O in surface/lattice
MgO(130)	200	1.91	122	all	0
	300	2.93	124	all	30% surface
	500	8.06	120	all	1.9 layers
	700	19.21	71	all	9.3 layers
	900	18.68	40		16 layers
MgO(390)	300	8.67	305	all	37% surface
	500	14.91	287	all	1.5 layers
	700	20.10	87	all	7.9 layers

---

(29) Itoh, H.; Utamapanya, S.; Klabunde, K. J.; Schlup, J. R. *J. Am Chem. Soc.*, submitted.

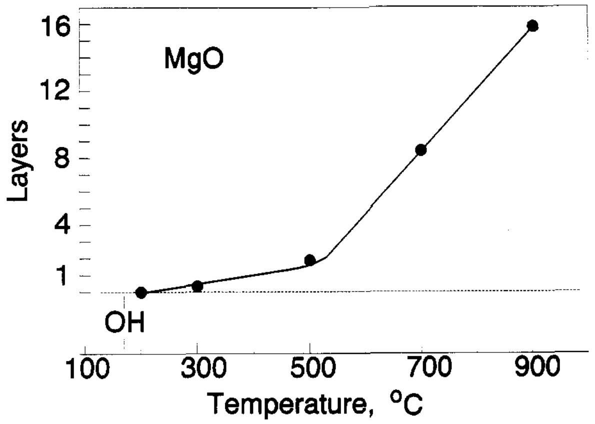

Figure 5. Exchangeability of lattice oxygen in MgO with water vapor vs temperature. There are two slopes, which indicates two sets of kinetic parameters in the exchange process: one is of lower activation energy, the other is of higher activation energy. On the basis of the amount of $H_2{}^{18}O$ exchanged at 500 °C, which is the changeover temperature, it can be determined from calculation that about 15% of the $Mg^{16}O$ moieties are capable of low activation exchange.

by steam and very high temperatures, has been observed before.[30,31]

These results are inverse to the D_2O results; higher temperatures cause more $^{16}O/^{18}O$ exchange in spite of the fact that the number of surface OH groups decreases. It is clear that lattice oxygen is also involved in the $^{16}O/^{18}O$ exchange. Furthermore, interior oxide anions must be involved since the amount of $^{16}O/^{18}O$ exchange is large compared with surface oxide available. In fact, calculations of f_{18}, coupled with the assumption that layers nearer the surface would be most susceptible to the $^{16}O/^{18}O$ exchange, showed that multilayer exchange takes place for both MgO(130) and MgO(390), even up to 16 layers deep at 900 °C for MgO(130) (see Table II).

It is important to note that the higher surface area MgO(390) at 300 and 500 °C (temperatures low enough so that severe sintering has not occurred) allows more $^{16}O/^{18}O$ exchange. This is a function of surface area, since when the amount is normalized, the percent of surface and the number of layers exchanged are comparable with MgO(130), as demonstrated in Table II. These calculations were based on the lower surface areas (measured after use, i.e., after exhaustive pulsing of labeled water). The surface area of one MgO moiety was taken as 8.86×10^{-20} m^2.[1]

It can be seen that at 300 °C the surface lattice ^{16}O began to exchange with $H_2{}^{18}O$. At 500 °C more than an entire layer of surface lattice ^{16}O was exchanged. At higher temperatures still more layers exchanged.

An interesting point is that both MgO(130) and MgO(390) yielded similar exchange depths at the same temperatures. Since these samples were prepared by very different methods, and the MgO(130) is much more crystalline than the MgO(390),[29,32] these results suggest that the exchange mechanism with $H_2{}^{18}O$ is not very sensitive to surface morphology. That is, the kinetics of exchange are probably dependent on surface area only, rather than defect site concentrations. If a rough plot of exchange depth vs temperature is made (Figure 5), it shows two slopes. This indicates that two different sets of kinetic parameters are possible, one probably for surface ^{16}O exchange, and one for deeper lattice ^{16}O, and the changeover point is about 500 °C.

Scheme I

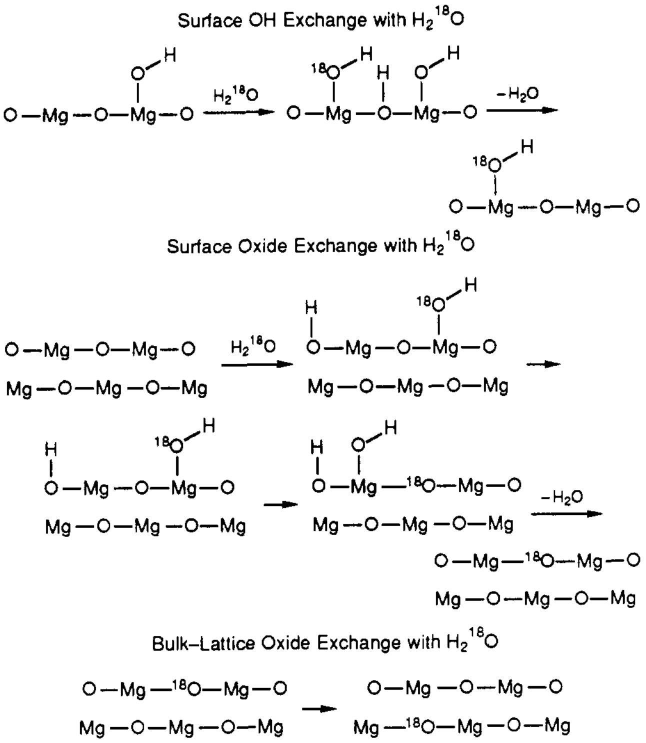

Similar results have been reported by Winter,[11] Boreskov,[15,33] and Harrison and co-workers[34] for isotopic exchange of ionic solids with diatomic gases (e.g., $Na^{36}Cl/Cl_2$ and $Zn^{16}O/^{18}O_2$). The surface process is of lower activation energy (type A) while bulk-lattice exchange is of higher activation energy (type B).

In our samples, these data, based on the amount of $H_2{}^{18}O$ exchanged at 500 °C, suggest that about 15% of the $Mg^{16}O$ moieties are capable of low E_a exchange. At higher temperature the exchange process becomes dominated by the E_a of oxide anion diffusion in the bulk and is about 5 times higher; that is, E_a(diffusion) is five times greater than E_a(exchange).

Regarding the mechanism of this $MgO/H_2{}^{18}O$ heterophasic exchange, it is helpful to consider possible mechanistic schemes for three regimes, as shown in Scheme I.

We should mention several important aspects of these findings:

(1) This is the first example of such $^{16}O/^{18}O$ exchange in ionic oxides using water as the exchange reagent.

(2) In the case of MgO and CaO, which are ionic solids without variable oxidation states, $H_2{}^{18}O$ works much better than $^{18}O_2$ according to comparative experiments we have carried out.

(3) This exchange process can be controlled with temperature so that only surface OH, or plus surface oxide, or plus bulk oxide can be exchanged.

(4) This process is quite effective for the preparation of ^{18}O-labeled metal oxides, and these are useful reagents for clarifying mechanistic details of surface adsorption/decomposition processes.

An example where an adsorption/decomposition process was clarified by the use of $Mg^{18}O$ is now discussed.

In continuing work on trying to understand the surface chemistry of the organophosphorus decomposition on

---

(30) Coluccia, S.; Tench, A. J.; Segall, R. L. *J. Chem. Soc., Faraday Trans. 1* **1979**, *75*, 1769.

(31) Morris, R. M. Ph.D. Thesis, University of North Dakota, **1981**.

(32) Utamapanya, S.; Klabunde, K. J.; Schlup, J. *Chem. Mater.* **1991**, *3*, 175.

(33) Boreskov, G. K. *Discuss. Faraday Soc.* **1966**, *41*, 263.

(34) Harrison, L. G.; Morrison, J. A. *J. Phys. Chem.* **1958**, *62*, 372.

Chem. Mater. **1992,** *4,* 615–619

Table III. DMMP Decomposition (atom percent) over $Mg^{18}O$: Labeled Formic Acid Formed

	$Mg^{18}O$(130)		$Mg^{18}O$(390)	
sample	HCOOH[a]	$HCO^{18}OH$[a]	HCOOH[a]	$HCO^{18}OH$[a]
on $Mg^{18}O$ sample saturated at 500 °C	66	34	33	67
on $Mg^{18}O$ sample saturated at 700 °C	63	37	34	66

[a] Decomposition products.

MgO,[1-3] we have shown that formic acid is a major product of the destructive adsorption of $(CH_3O)_2P(O)CH_3$(DMMP) on MgO. A question arises as to where the oxygen comes from in order to oxidize adsorbed OCH_3 groups to formic acid.

At 500 and 700 °C the $Mg^{18}O$(130) and $Mg^{18}O$(390) were pulsed with 1-μL portions of DMMP, and the formic acid released was monitored by GC-MS. The formic acid was found to be partly labeled with ^{18}O (Table III). The ^{18}O label could only have come from the $Mg^{18}O$, since no $H_2{}^{18}O$ was added to the DMMP pulses. Therefore, large portions of surface/lattice ^{18}O were taken up to form formic acid. This oxygen was replaced, we believe, by oxygen donation from other molecules of DMMP, probably as follows:

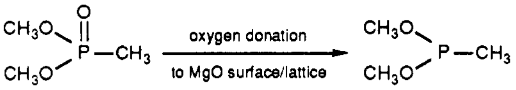

In general, our experiments suggest that surface/lattice oxide is likely to be involved in a wide variety of adsorption/decomposition processes.

Acknowledgment. The support of the Army Research Office is acknowledged with gratitude.

Registry No. DMMP, 756-79-6; HO, 7732-18-5; MgO, 1309-48-4; CaO, 1305-78-8; Fe_2O_3, 1309-37-1.

Preparation and Characterization of $Cd_{1-x}Hg_xSe$ Thin Films

Shixing Weng and Michael Cocivera*

Guelph Waterloo Centre for Graduate Work in Chemistry, University of Guelph, Guelph, Ontario, Canada, N1G 2W1

Received November 7, 1991. Revised Manuscript Received January 3, 1992

Thin-film $Cd_{1-x}Hg_xSe$ was deposited on indium/tin oxide coated glass (ITO) by electrochemical reduction of an aqueous solution containing Cd^{2+}, Hg^{2+}, and $SeSO_3{}^{2-}$. Deposition potential and Hg^{2+} concentration in the deposition solution affected the composition of the film. Proton-induced X-ray emission showed that x could be varied from 0.074 to 0.45 by adjusting the deposition potential. The Hg composition could also be altered by varying the Hg^{2+} concentration in the solution. The effect of composition on the bandgap of the film was determined by optical absorption spectra and was found to decrease as the Hg content increased. Annealing at 320 °C caused the bandgap to shift to higher energy; at this maximum temperature significant loss of Hg was observed. X-ray diffraction confirmed that the crystallite size increased significantly upon annealing the film, and scanning electron microscopy showed that these films were free of cracks and pinholes.

Introduction

CdSe is an n-type semiconductor with the minimum bandgap energy about 1.7 eV, which is suitable for solar cell applications.[1] HgSe alloy is a semimetal with the minimum bandgap energy that is essentially zero.[2] Consequently, the minimum bandgap energy of the $Cd_{1-x}Hg_xSe$ (CMS), in principle, can be varied between 0 and 1.7 eV by varing the Cd:Hg ratio.[3] This flexibility provides the possibility for various practical applications ranging from infrared detection to solar energy conversion. For solar cell applications the optimum bandgap energy is in the range 1.0–1.6 eV,[4] which can be achieved by adjusting the composition of CMS.

A few methods have been reported for preparing CMS. Single crystals of CMS were grown by the Bridgman method.[5] Recently, thin-film CMS has been grown epitaxially on CdSe substrates.[6] Nelson et al.[2] studied the electron mobility of the single-crystal compounds with the mole fraction of Hg ranging from 0.88 to 0.32 in the temperature range 4.2–300 K. They determined that the CMS semiconductor was n-type and that the electronic conduction was dominated by intrinsic and defect scattering mechanisms.

The present report describes an electrochemical reduction method for making CMS semiconducting thin films. The approach is similar to the one used in our laboratory to make polycrystalline thin-film CdSe.[7] One of the goals of this work was to ascertain if solution composition and/or deposition potential could be employed to control the Hg content in the CMS film and also determine if the film was a uniform alloy or a composite of CdSe and HgSe crystals. Another goal was to determine the effect of annealing temperature on the composition and bandgap of the film. In addition we wished to explore the effect of heat treatment on crystal structure and surface morphology of the film and obtain some preliminary information about the conductivity of this material.

---

* Address correspondence to this author.

(1) Fahrenbruch, A. L.; Bube, R. H. *Fundamentals of Solar Cells*; Academic Press, Toronto, 1983.

(2) Lehoczky, S. L.; Broerman, J. G.; Nelson, J. G.; Whitsett, C. R. *Phys. Rev. B* **1974**, *9*, 1598.

(3) Nelson, D. A.; Broerman, J. G.; Summers, C. J.; Whitsett, C. R. *Phys. Rev. B* **1978**, *18*, 1658.

(4) Prince, M. B. *J. Appl. Phys.* **1955**, *26*, 534.

(5) Broerman, J. G. *Proceedings of the Eleventh International Conference on the Physics of Semiconductors*; Polish Scientific: Warsaw, 1972; Vol. 2, 917.

(6) Kong, H. Z.; Shi, W. D.; Wang, D. C.; Wang, B. K. *Chin. Phys.* (Engl. Ed.) **1988**, *8*, 804.

(7) Szabo, J. P.; Cocivera, M. *J. Electrochem. Soc.* **1986**, *133*, 1247.

0897-4756/92/2804-0615$03.00/0